

Bayesian reconstruction of past land-cover from pollen data: model robustness and sensitivity to auxiliary variables

Behnaz Pirzamanbein ^{*1,2,3}, Johan Lindström¹ and Anneli Poska^{4,5}

¹Department of Applied Mathematics and Computer Science, Technical University of Denmark

²Centre for Mathematical Sciences, Lund University, Sweden

³Centre for Environmental and Climate Research, Lund University, Sweden

⁴Department of Physical Geography and Ecosystems Analysis, Lund University, Sweden

⁵Institute of Geology, Tallinn University of Technology, Estonia

Abstract

Realistic depictions of past land cover are needed to investigate prehistoric environmental changes, effects of anthropogenic deforestation, and long term land cover-climate feedbacks. Observation based reconstructions of past land cover are rare and commonly used model based reconstructions exhibit considerable differences. Recently Pirzamanbein et al. (*Spatial Statistics*, 24:14–31, 2018) developed a statistical interpolation method that produces spatially complete reconstructions of past land cover from pollen assemblage. These reconstructions incorporate a number of auxiliary datasets raising questions regarding the method’s sensitivity to different auxiliary datasets.

Here the sensitivity of the method is examined by performing spatial reconstructions for northern Europe during three time periods (1900 CE, 1725 CE and 4000 BCE). The auxiliary datasets considered include the most commonly utilized sources of past land-cover data — e.g. estimates produced by a dynamic vegetation (DVM) and anthropogenic land-cover change (ALCC) models. Five different auxiliary datasets were considered, including different climate data driving the DVM and different ALCC models. The resulting reconstructions were also evaluated using cross-validation for all the time periods. For the recent time period, 1900 CE, the different land-cover reconstructions were compared against a present day forest map.

The validation confirms that the statistical model provides a robust spatial interpolation tool with low sensitivity to differences in auxiliary data and high capacity to capture information in the pollen based proxy data. Further auxiliary data with high spatial detail improves model performance for areas with complex topography or few observations.

*Corresponding author: Behnaz Pirzamanbein, bepi@dtu.dk

1 Introduction

The importance of terrestrial land cover for the global carbon cycle and its impact on the climate system is well recognized (e.g. Claussen et al., 2001; Brovkin et al., 2006; Arneth et al., 2010; Christidis et al., 2013). Many studies have found large climatic effects associated with changes in land cover. Forecast simulations evaluating the effects of human induced global warming predict a considerable amplification of future climate change, especially for Arctic areas (Zhang et al., 2013; Richter-Menge et al., 2011; Chapman and Walsh, 2007; Koenigk et al., 2013; Miller and Smith, 2012). The past anthropogenic deforestation of the temperate zone in Europe was lately demonstrated to have an impact on regional climate similar in amplitude to present day climate change (Strandberg et al., 2014). However, studies on the effects of vegetation and land-use changes on past climate and carbon cycle often report considerable differences and uncertainties in their model predictions (de Noblet-Ducoudré et al., 2012; Olofsson, 2013).

One of the reasons for such widely diverging results could be the differences in past land-cover descriptions used by climate modellers. Possible land-cover descriptions range from static present-day land cover (Strandberg et al., 2011), over simulated potential natural land cover from dynamic (or static) vegetation models (DVMs) (e.g. Brovkin et al., 2002; Hickler et al., 2012), to past land-cover scenarios combining DVM derived potential vegetation with estimates of anthropogenic land-cover change (ALCC) (Strandberg et al., 2014; Pongratz et al., 2008; de Noblet-Ducoudré et al., 2012). Differences in input climates, mechanistic and parametrisation differences of DVMs (Prentice et al., 2007; Scheiter et al., 2013), and significant variation between existing ALCC scenarios (e.g. Kaplan et al., 2009; Pongratz et al., 2008; Goldewijk et al., 2011; Gaillard et al., 2010) further contribute to the differences in past land-cover descriptions. These differences can lead to largely diverging estimates of past land-cover dynamics even when the most advanced models are used (Strandberg et al., 2014; Pitman et al., 2009). Thus, reliable land-cover representations are important when studying biogeophysical impacts of anthropogenic land-cover change on climate.

The palaeoecological proxy based land-cover reconstructions recently published by Pirzamanbein et al. (2014, 2018) were designed to overcome the problems described above. And to provide a proxy based land-cover description applicable for a range of studies on past vegetation and its interactions with climate, soil and humans. These reconstructions use the pollen based land-cover composition (PbLCC) published by Trondman et al. (2015) as a source of information on past land-cover composition. The PbLCC are point estimates, depicting the land-cover composition of the area surrounding each of the studied sites. Spatial interpolation is needed to fill the gaps between observations and to

produce continuous land-cover reconstructions. Conventional interpolation methods might struggle when handling noisy, spatially heterogeneous data (Heuvelink et al., 1989; de Knecht et al., 2010), but statistical methods for spatially structured data exist (Gelfand et al., 2010; Blangiardo and Cameletti, 2015).

In Pirzamanbein et al. (2018) a statistical model based on Gaussian Markov Random Fields (Lindgren et al., 2011; Rue and Held, 2005) was developed to provide a reliable, computationally effective and freeware based spatial interpolation technique. The resulting statistical model combines PbLCC data with auxiliary datasets; e.g. DVM output, ALCC scenarios, and elevation; to produce reconstructions of past land cover. The auxiliary data is subject to the differences and uncertainties outlined above and the choice of auxiliary data could influence the accuracy of the statistical model. The major objectives of this paper are: 1) To draw attention of climate modelling community to a novel set of spatially explicit pollen-proxy based land-cover reconstructions suitable for climate modelling; 2) to present and test the robustness of the spatial interpolation model developed by Pirzamanbein et al. (2018); and 3) to evaluate the models capacity to recover information provided by PbLCC proxy data and to analyse its sensitivity to different auxiliary datasets.

2 Material and Methods

The studied area covers temperate, boreal and alpine-arctic biomes of central and northern Europe (45°N to 71°N and 10°W to 30°E). The PbLCC data published in Trondman et al. (2015) consists of proportions of coniferous forest, broadleaved forest and unforested land presented as gridded ($1^\circ \times 1^\circ$) data points placed irregularly across northern-central Europe. Altogether 175 grid cells containing proxy data were available for 1900 CE, 181 for 1725 CE, and 196 for the 4000 BCE time-period (Figure 1, column 2).

Four different model derived datasets, depicting past land cover, along with elevation were considered as potential auxiliary datasets. In each case potential natural vegetation composition estimated by the DVM LPJ-GUESS (Lund-Potsdam-Jena General Ecosystem Simulator; Smith et al., 2001; Sitch et al., 2003) were combined with an ALCC scenario to adjust for human land use (see Pirzamanbein et al., 2014, for details):

K-LRCA3: Combines the ALCC scenario KK10 (Kaplan et al., 2009) and the potential natural vegetation from LPJ-GUESS. Climate forcing for the DVM was derived from RCA3 (Rossby Centre Regional Climate Model, Samuelsson et al., 2011) at annual time and $0.44^\circ \times 0.44^\circ$ spatial resolution (Figure 1, column 3),

K-L_{ESM}: Combines the ALCC scenario KK10 and the potential natural vegetation from LPJ-GUESS.

Climate forcing for the DVM was derived from the Earth System Model (ESM; Mikolajewicz et al., 2007) at centennial time and $5.6^\circ \times 5.6^\circ$ spatial resolution. To interpolate data into annual time and $0.5^\circ \times 0.5^\circ$ spatial resolution climate data from 1901–1930 CE provided by the Climate Research Unit was used (Figure 1, column 4),

H-L_{RCA3}: Combines the ALCC scenario from the History Database of the Global Environment (HYDE; Goldewijk et al., 2011) and vegetation from LPJ-GUESS with RCA3 climate forcing (Figure 1, column 5),

H-L_{ESM}: Combines the ALCC scenario from HYDE and vegetation from LPJ-GUESS with ESM climate forcing (Figure 1, column 6).

The elevation data (denoted $\text{SRTM}_{\text{elev}}$) was obtained from the Shuttle Radar Topography Mission (Becker et al., 2009) (Figure 1, column 1 row 2).

Finally, a modern forest map based on data from the European Forest Institute (EFI) is used for evaluation of the model’s performance for the 1900 CE time period. The EFI forest map (EFI-FM) is based on a combination of satellite data and national forest-inventory statistics from 1990–2005 (Pivinen et al., 2001; Schuck et al., 2002) (Figure 1, column 1 row 1). All auxiliary data were up-scaled to $1^\circ \times 1^\circ$ spatial resolution, matching the pollen based reconstructions, before usage as model input.

2.1 Statistical Model for Land-cover Compositions

A Bayesian hierarchical model is used to interpolate the PbLCC data; here we only provide a brief overview of the model, mathematical and technical details can be found in Pirzamanbein et al. (2018). The model can be seen as a special case of a generalized linear mixed model with a spatially correlated random effect. An alternative interpretation of the model is as an empirical forward model (direction of arrows in Figure 2) where parameters affect the latent variables which in turn affect the data. Reconstructions are obtained by inverting the model (i.e. computing the posterior) to obtain the latent variables given the data.

The PbLCC derived proportions of land cover (coniferous forest, broadleaved forest and unforested land), denoted $\mathbf{Y}_{\text{PbLCC}}$, are seen as draws from a Dirichlet distribution (Kotz et al., 2000, Ch. 49) given a vector of proportions, \mathbf{Z} , and a concentration parameter, α (controlling the uncertainty: $\mathbf{V}(\mathbf{Y}_{\text{PbLCC}}) \propto 1/\alpha$). Since the proportions have to obey certain restrictions ($0 \leq Z_k \leq 1$ and $\sum_{k=1}^3 Z_k = 1$, where k indexes the land-cover types), a link function is used to transform between the

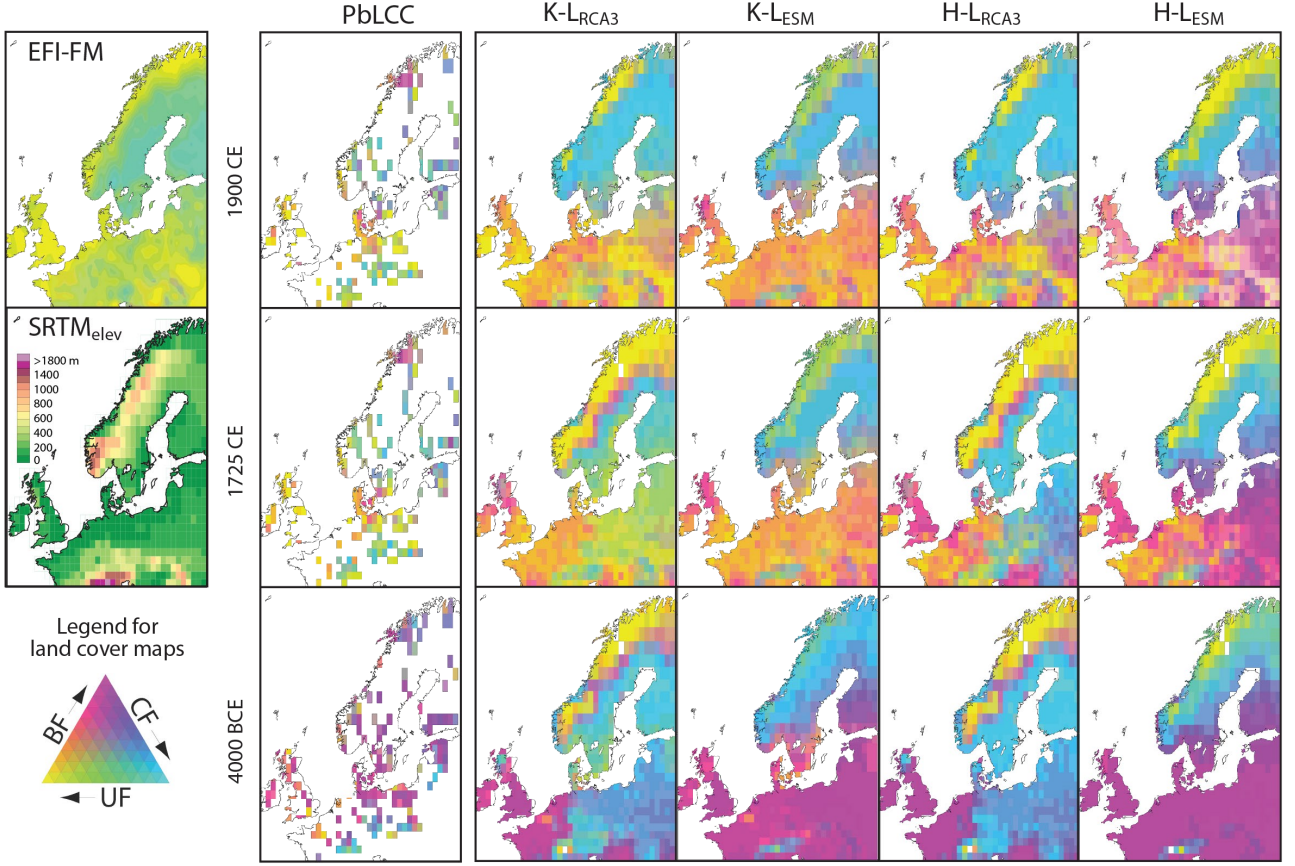


Figure 1: Data used in the modelling. The first column shows (from top to bottom) the EFI-FM, $SRTM_{elev}$, and the colorkey for the land-cover compositions, coniferous forest (CF), broadleaved forest (BF) and unforested land (UF). The remaining columns give (from left to right) the PbLCC (Trondman et al., 2015) and the four model based compositions considered as potential covariates: K-L_{RCA3}, K-L_{ESM}, H-L_{RCA3}, and H-L_{ESM}. Here K/H indicates KK10 (Kaplan et al., 2009) or HYDE (Goldewijk et al., 2011) land use scenarios and L_{RCA3}/L_{ESM} indicates the climate — Rossby Centre Regional Climate Model (Samuelsson et al., 2011) or Earth System Model (Mikolajewicz et al., 2007) — used to drive the vegetation model. The three rows represent (from top to bottom) the time periods 1900 CE, 1725 CE, and 4000 BCE.

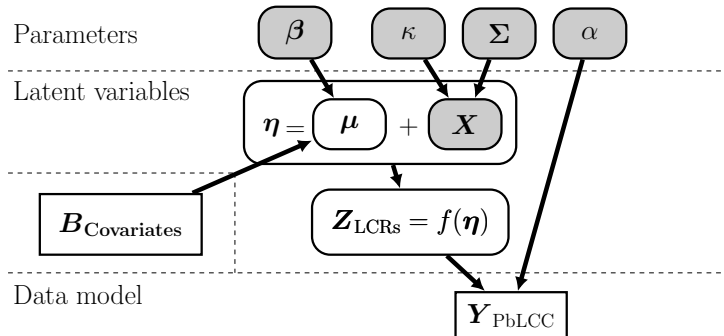


Figure 2: Hierarchical graph describing the conditional dependencies between observations (white rectangle) and parameters (grey rounded rectangles) to be estimated. The white rounded rectangles are computed based on the estimations. In a generalized linear mixed model framework, $\boldsymbol{\eta}$ is the linear predictor — consisting of a regression term, $\boldsymbol{\mu}$, and a spatial random effect, \mathbf{X} . The link function, $f(\boldsymbol{\eta})$, transforms between linear predictor and proportions, which are matched to the observed land cover proportions, \mathbf{Y}_{PbLCC} , using a Dirichlet distribution.

Table 1: Six different models and corresponding covariates. $\text{SRTM}_{\text{elev}}$ is elevation (Becker et al., 2009), K/H indicates KK10 (Kaplan et al., 2009) or HYDE (Goldewijk et al., 2011) land use scenarios and $\text{L}_{\text{RCA3}}/\text{L}_{\text{ESM}}$ indicates vegetation model driven by climate from the Rossby Centre Regional Climate Model (Samuelsson et al., 2011) or from an Earth System Model (Mikolajewicz et al., 2007).

Covariates Model	Intercept	$\text{SRTM}_{\text{elev}}$	K- L_{ESM}	K- L_{RCA3}	H- L_{ESM}	H- L_{RCA3}
Constant	x					
Elevation	x	x				
K- L_{ESM}	x	x	x			
K- L_{RCA3}	x	x		x		
H- L_{ESM}	x	x			x	
H- L_{RCA3}	x	x				x

proportions and the linear predictor, $\boldsymbol{\eta}$:

$$Z_k = f(\boldsymbol{\eta}) = \begin{cases} \frac{e^{\eta_k}}{1 + \sum_{i=1}^2 e^{\eta_i}} & \text{for } k = 1, 2 \\ \frac{1}{1 + \sum_{i=1}^2 e^{\eta_i}} & \text{for } k = 3 \end{cases}$$

$$\eta_k = f^{-1}(\mathbf{Z}) = \log\left(\frac{Z_k}{Z_3}\right) \quad \text{for } k = 1, 2$$

Here $f^{-1}(\mathbf{Z})$ is the additive log-ratio transformation (Aitchison, 1986), a multivariate extension of the logit transformation.

The linear predictor consists of a mean structure and a spatially dependent random effect, $\boldsymbol{\eta} = \boldsymbol{\mu} + \mathbf{X}$. The mean structure is modelled as a linear regression, $\boldsymbol{\mu} = \mathbf{B}\boldsymbol{\beta}$; i.e. a combination of covariates, \mathbf{B} , and regression coefficients, $\boldsymbol{\beta}$. To aid in variable selection and suppress uninformative covariates a horseshoe prior (Park and Casella, 2008; Makalic and Schmidt, 2016) is used for $\boldsymbol{\beta}$. The main focus of this paper is to evaluate the model sensitivity to the choice of covariates (i.e. the auxiliary datasets). The PbLCC is modelled based on six different sets of covariates: 1) Intercept, 2) $\text{SRTM}_{\text{elev}}$, 3) K- L_{ESM} , 4) K- L_{RCA3} , 5) H- L_{ESM} , and 6) H- L_{RCA3} ; illustrated in Figure 1. A summary of the different models is given in Table 1.

Finally, the spatially dependent random effect is modelled using a Gaussian Markov Random Field (Lindgren et al., 2011) with two parameters: κ , controlling the strength of the spatial dependence and $\boldsymbol{\Sigma}$, controlling the variation within and between the fields (i.e. the correlation among different land cover types).

Model estimation and reconstructions are performed using Markov Chain Monte Carlo (Brooks et al., 2011) with 100 000 samples and a burn-in of 10 000 (See Pirzamanbein et al., 2018, for details.). Output from the Markov Chain Monte Carlo are then used to compute land-cover reconstructions

(as posterior expectations, $E(\mathbf{Z}|\mathbf{Y}_{\text{pBLCC}})$) and uncertainties in the form of predictive regions. The predictive regions describe the uncertainties associated with the reconstructions; including uncertainties in model parameters and linear predictor.

2.2 Testing the Model Performance

To evaluate model performance, we compared the land-cover reconstructions from different models for the 1900 CE time period with the EFI-FM by computing the average compositional distances (Aitchison et al., 2000; Pirzamanbein et al., 2018). This measure is similar to root mean square error in \mathbb{R}^2 but it accounts for compositional properties (i.e. $0 \leq Z_k \leq 1$ and $\sum_{k=1}^3 Z_k = 1$).

Since no independent observational data exists for the 1725 CE and 4000 BCE time periods, we applied a 6-fold cross-validation scheme (Hastie et al., 2001, Ch. 7.10) to all models and time periods. The cross-validation divides the observations into 6 random groups and the reconstruction errors for each group when using only observations from the other 5 groups are computed. To further compare predictive performance of the models Deviance Information Criteria (DIC; see Ch. 7.2 in Gelman et al., 2014) were computed for all models and time periods. The DIC is a hierarchical modelling generalization of the Akaike and Bayesian information criteria (Hastie et al., 2001, Ch. 7).

3 Results and Discussion

Fossil pollen is a well-recognized information source of vegetation dynamics and generally accepted as the best observational data on past land-cover composition and environmental conditions (Trondman et al., 2015).

Today, central and northern Europe have, at the subcontinental spatial scale, the highest density of palynologically investigated sites on Earth. However, even there the existing pollen records are irregularly placed, leaving some areas with scarce data coverage (Fyfe et al., 2015). The collection of new pollen data to fill these gaps is very time consuming and cannot be performed everywhere. All this makes pollen data, in their original format, heavily underused, since the data is unsuitable for models requiring continuous land-cover representations as input. The lack of spatially explicit proxy based land cover data directly usable in climate models has been hampering the correct representation of past climate-land cover relationship.

Regrettably, the commonly used DVM derived representations of past land cover exhibit large variation in vegetation composition estimates. The model derived land-cover datasets used as auxiliary data (Table 1) show large variation in estimated extents of coniferous and broadleaved forests, and

unforested areas for all of the studied time periods (Figure 1). These substantial differences illustrate large deviances between model based estimates of the past land-cover composition due to differences in applied climate forcing and/or ALCC scenarios. Differences in climate model outputs (Harrison et al., 2014; Gladstone et al., 2005) and ALCC model estimates (Gaillard et al., 2010) have been recognized in earlier comparison studies and syntheses. The effect of the differences in input climate forcing and ALCC scenario on DVM estimated land-cover composition presented here are especially pronounced for central and western Europe, and for elevated areas in northern Scandinavia and the Alps (Figure 1). In general the KK10 ALCC scenario produces larger unforested areas, notably in western Europe, compared to the HYDE scenario. Compared to the ESM climate forcing; the RCA3 forcing results in higher proportions of coniferous forest, especially for central, northern and eastern Europe. The described differences are clearly recognizable for all the considered time periods and are generally larger between time periods than within each time period. The purpose of the statistical model presented in Section 2.1 is to combine the observed PbLCC with the spatial structure in the auxiliary data to produce data driven spatially complete maps of past land-cover that can be used directly (as input) in others models.

To illustrate the structure of the statistical model, step by step advancement from auxiliary data (model derived land cover) to final statistical estimates of land cover compositions for 1725 CE are given in Figures 3 and 4. The large differences in K-L_{RCA3} and K-L_{ESM} are reduced by scaling with the regression coefficients, β , capturing the empirical relationship between covariates and PbLCC data. Thereafter, the land-cover estimates are subjected to similar adjustments due to intercept and SRTM_{elev}, and finally similar spatial dependent effects.

The impact of different auxiliary datasets was assessed by using the statistical model to create a set of proxy based reconstructions of past land cover for central and northern Europe during three time periods (1900 CE, 1725 CE and 4000 BCE; see Figures 5 and 6). Each of these reconstructions were based on the irregularly distributed observed pollen data (PbLCC), available for ca 25% of the area, together with one of the six models (Table 1) using different combinations of the auxiliary data (Figure 1).

The resulting land-cover reconstructions exhibit considerably higher similarity with the PbLCC data than any of the auxiliary land-cover datasets for all tested models and time periods (Figures 5 and 6). At first the similarity among the reconstructions might seem contradictory, but recall that the model allows for, and estimates, different weighting (the regression coefficients, β :s) for each of the auxiliary datasets. Thus, the resulting reconstructions do not rely on the absolute values in the auxiliary datasets, only their spatial patterns. As a result, model performance for elevated areas and

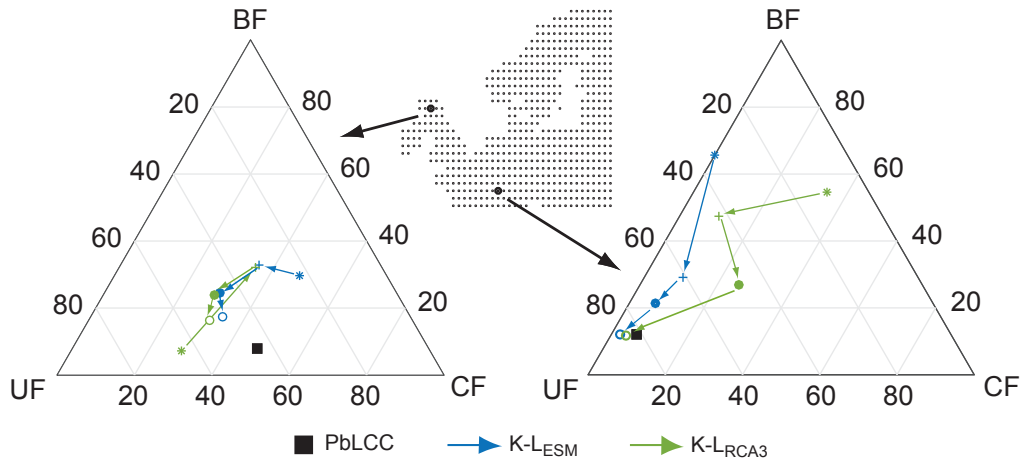


Figure 3: Advancement of the model for two locations at 1725 CE. Starting from the value of the $K-L_{RCA3}$ and $K-L_{ESM}$ covariates (*), the cumulative effects of regression coefficients, β , (+); the intercept and $SRTM_{elev}$ covariates (\bullet); and, finally, the spatial dependency structures (\circ), are illustrated. With the final points (\circ) corresponding to the land-cover reconstructions and \blacksquare marking the observed pollen based land-cover composition.

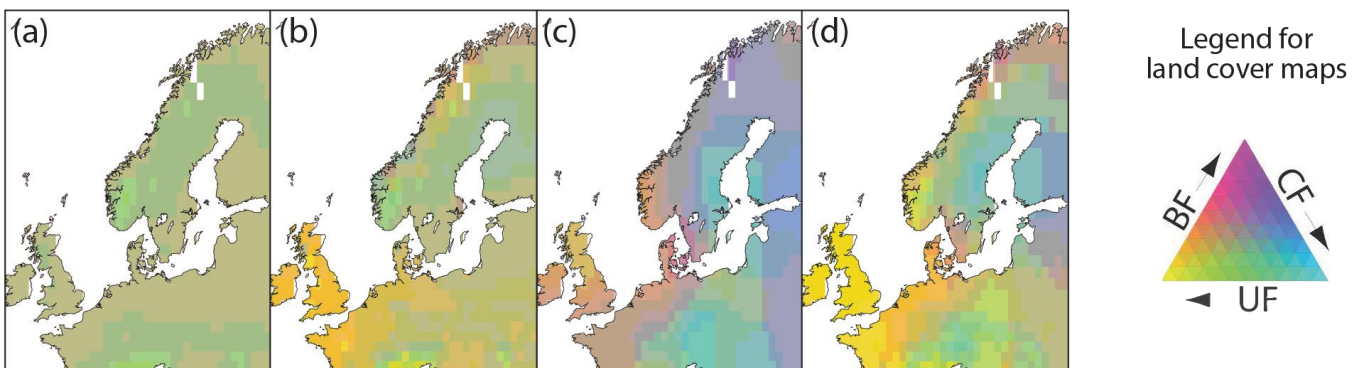


Figure 4: Advancement of $K-L_{ESM}$ models for the 1725 CE time period: (a) shows the effect of intercept and $SRTM_{elev}$, (b) shows the mean structure, μ , including all the covariates, (c) shows the spatial dependency structure and finally (d) shows the resulting land-cover reconstructions obtained by adding (b) and (c).

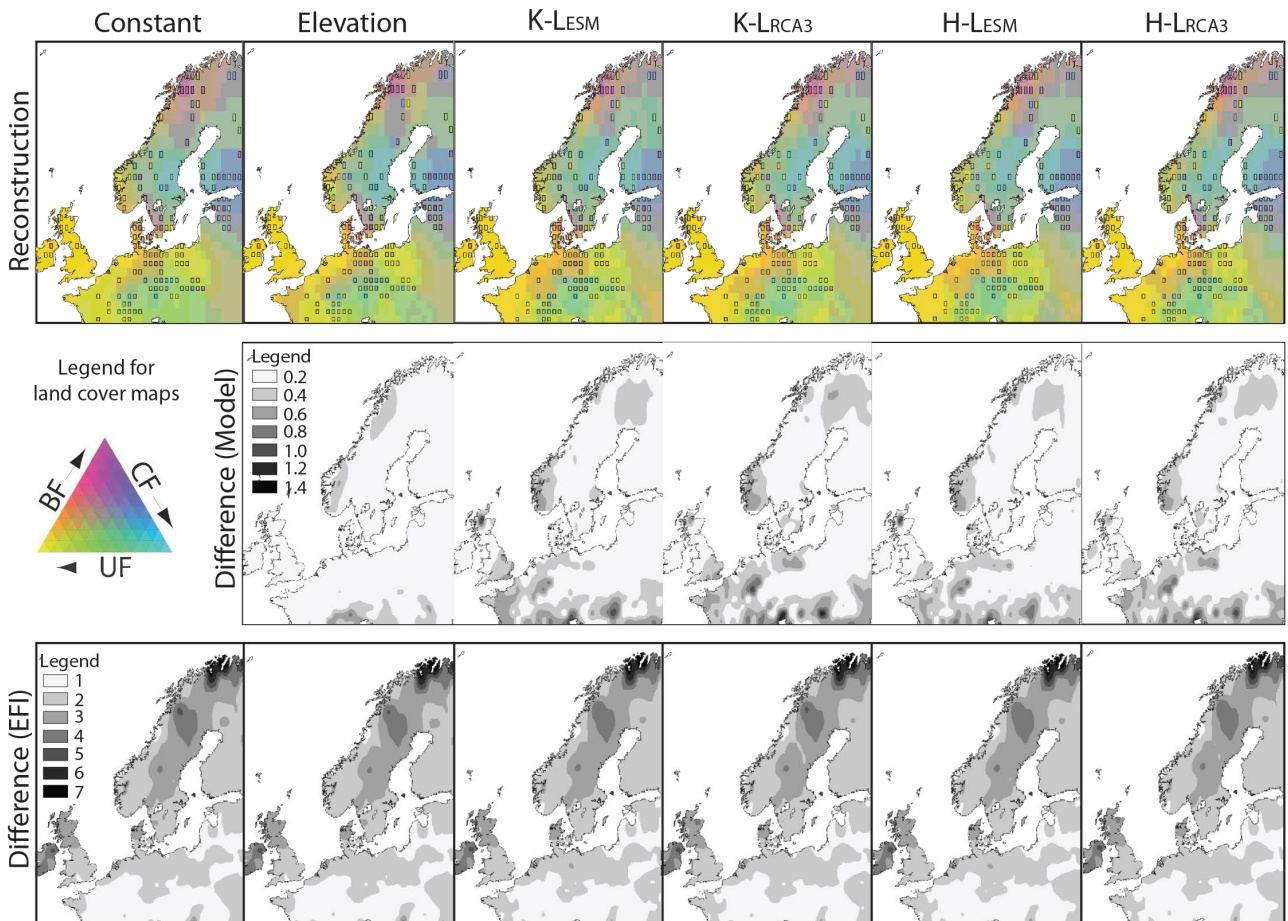


Figure 5: Land-cover reconstructions using PbLCC for the 1900 CE time periods (top row). The reconstructions are based on six different models (see Table 1) with different auxiliary datasets. Locations and compositional values of the available PbLCC data are given by the black rectangles. Middle row shows the compositional distances between each model and the Constant model. Bottom row shows the compositional distances between each model and the EFI-FM.

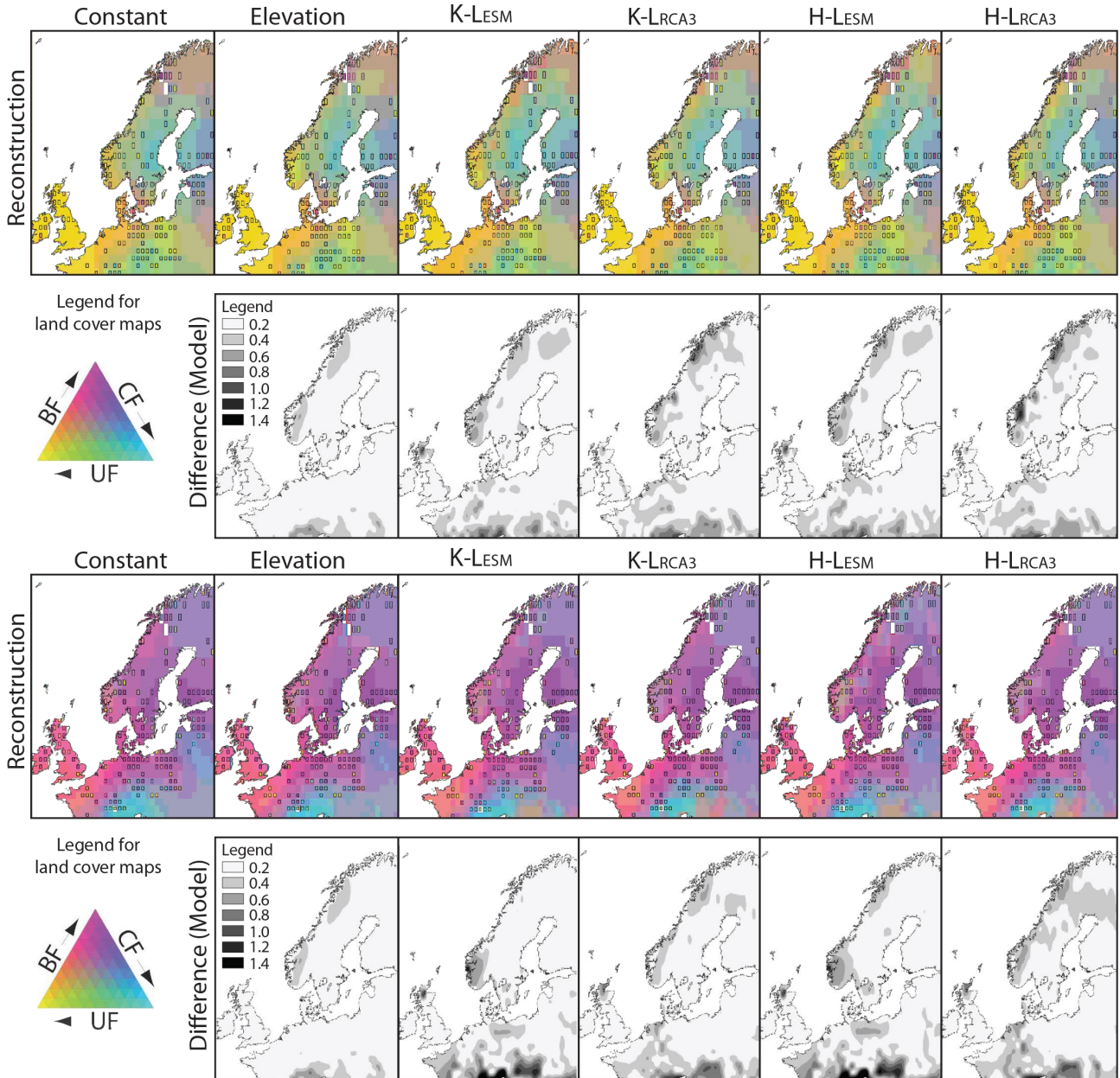


Figure 6: Land-cover reconstructions using local estimates of PbLCC for the 1725 CE (top) and 4000 BCE (bottom) time periods. The reconstructions are based on six different models (see Table 1) with different auxiliary datasets. Locations and compositional values of the available PbLCC data are given by the black rectangles. Third and fourth row show the compositional distances between each model and the Constant model.

for the areas with low observational data coverage (e.g. eastern and south-eastern Europe) is improved by including covariates that exhibit distinct spatial structures for the given areas (Figures 5 and 6). Neither the DIC results nor the 6-fold cross-validation results show any advantage among the six tested models for the different time periods (Table 2). Analogous to the reconstructions, the predictive regions are very similar in both size and shape irrespective of the auxiliary dataset used, indicating similar reconstruction uncertainties across all models (Figure 7). Implying there is no clear preference among the models, i.e. that the results are robust to the choice of auxiliary dataset.

	DIC			ACD		
	1900CE	1725CE	4000BCE	1900CE	1725CE	4000BCE
Constant	-559	-655	-593	1.00	1.12	1.20
Elevation	-568	-664	-589	0.99	1.11	1.21
K-L _{ESM}	-547	-649	-609	1.00	1.12	1.18
K-L _{RCA3}	-549	-661	-589	0.99	1.13	1.19
H-L _{ESM}	-549	-655	-608	0.99	1.11	1.17
H-L _{RCA3}	-557	-669	-595	0.99	1.12	1.18

Table 2: Deviance information criteria (DIC) and Average compositional distances (ACD) from 6-fold cross-validations for each of the six models and three time periods. Best value for each time period marked in **bold-font**.

Although a temporal misalignment exists between the PbLCC data for the 1900 CE time period (based on pollen data from 1850 to the present) and the EFI-FM (inventory and satellite data from 1990-2005); EFI-FM provides the best complete and consistent land cover map of Europe for present time, making it a reasonable choice for a comparison. The main differences between the EFI-FM and the PbLCC data for the 1900 CE time period are: 1) lower abundance of broadleaved forests for most of Europe, 2) higher abundance of coniferous forest in Sweden and Finland, and 3) higher abundance of unforested land in North Norway in the EFI-FM data than in the PbLCC data (Pirzamanbein et al., 2018). The average compositional distances computed between the land-cover reconstructions and the EFI-FM for 1900 CE show practically identical (1.47 to 1.48) distances between all six reconstructions and the EFI-FM, and small differences among the six presented models (Table 3).

These results clearly show that the developed statistical interpolation model is robust to the choice of covariates. The model is suitable for reconstructing spatially continuous maps of past land cover from scattered and irregularly spaced pollen based proxy data.

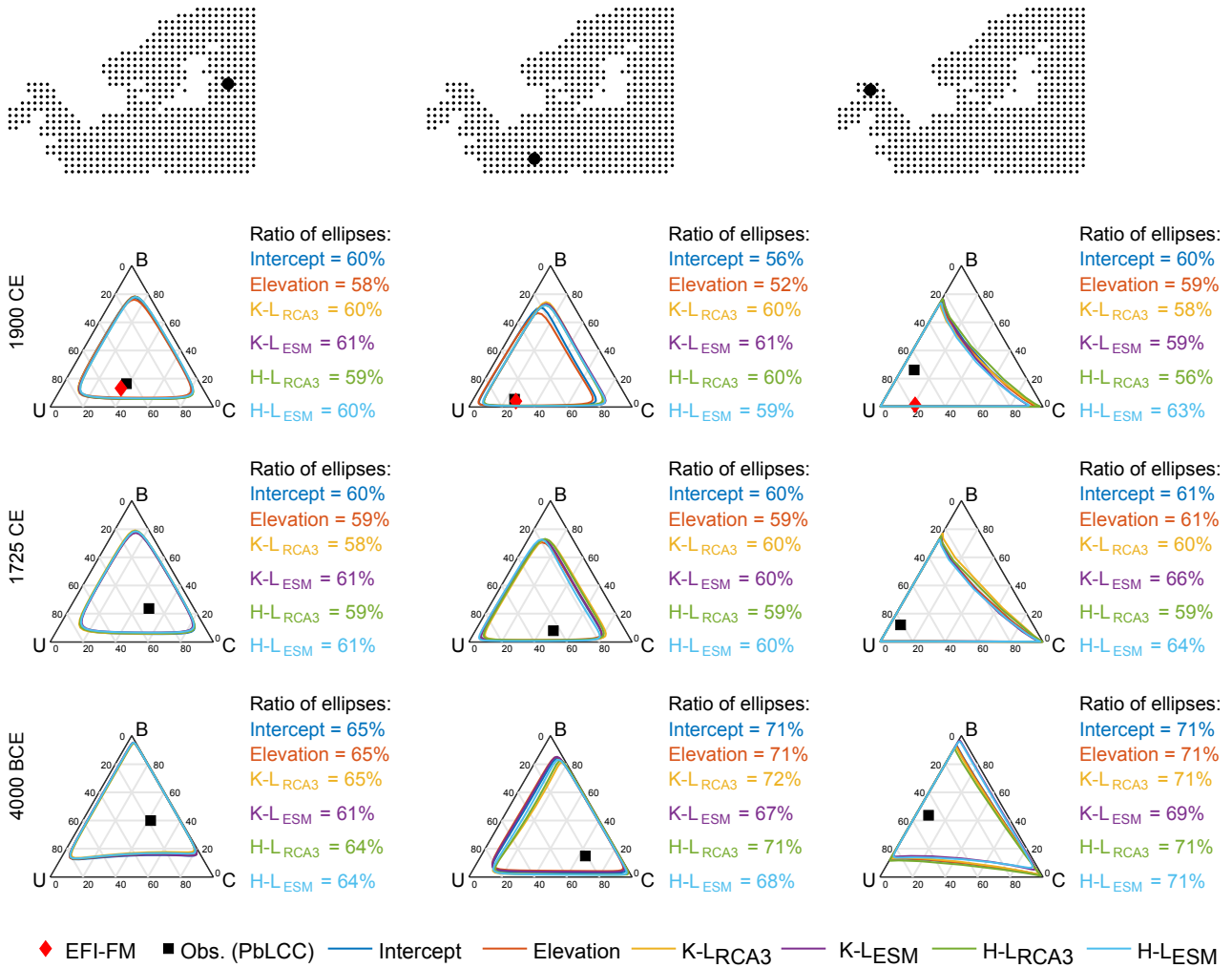


Figure 7: The prediction regions and fraction of the ternary triangle covered by these regions are presented for three locations, the six models, and the 1900 CE, 1725 CE and 4000 BCE time periods.

	EFI-FM	Elevation	K-L _{ESM}	K-L _{RCA3}	H-L _{ESM}	H-L _{RCA3}
1900 CE						
Constant	1.48	0.08	0.18	0.20	0.17	0.19
Elevation	1.49		0.19	0.21	0.18	0.20
K-L _{ESM}	1.48			0.09	0.07	0.09
K-L _{RCA3}	1.48				0.11	0.06
H-L _{ESM}	1.48					0.08
H-L _{RCA3}	1.48					
1725 CE						
Constant	0.10	0.16	0.16	0.17	0.17	
Elevation		0.14	0.11	0.14	0.13	
K-L _{ESM}			0.14	0.06	0.16	
K-L _{RCA3}				0.15	0.07	
H-L _{ESM}					0.15	
4000 BCE						
Constant	0.11	0.21	0.17	0.22	0.19	
Elevation		0.19	0.12	0.20	0.15	
K-L _{ESM}			0.19	0.07	0.21	
K-L _{RCA3}				0.18	0.07	
H-L _{ESM}					0.20	

Table 3: The average compositional distances among the six models fitted to the data for each of the three time periods.

4 Conclusions

The statistical model and Bayesian interpolation method presented here has been specially designed for handling irregularly spaced palaeo-proxy records like pollen data and, dependent on proxy data availability, is globally applicable. The model produces land-cover maps by combining irregularly distributed pollen based estimates of land cover with auxiliary data and a statistical model for spatial structure. The resulting maps capture important features in the pollen proxy data and are reasonably insensitive to the use of different auxiliary datasets.

Auxiliary datasets considered were compiled from commonly utilized sources of past land-cover data (outputs from a dynamic vegetation model using different climatic drivers and anthropogenic land-cover changes scenarios). These datasets exhibit considerable differences in their recreation of the past land cover. Emphasizing the need for the independent, proxy based past land-cover maps created in this paper.

Evaluation of the model’s sensitivity indicates that the proposed statistical model is robust to the choice of auxiliary data and only considers features in the auxiliary data that are consistent with the proxy data. However, auxiliary data with detailed spatial information considerably improves the interpolation results for areas with low proxy data coverage, with no reduction in overall performance.

This modelling approach has demonstrated a clear capacity to produce empirically based land-

cover reconstructions for climate modelling purposes. Such reconstructions are necessary to evaluate anthropogenic land-cover change scenarios currently used in climate modelling and to study past interactions between land cover and climate with greater reliability. The model will also be very useful for producing reconstructions of past land cover from the global pollen proxy data currently being produced by the PAGES (Past Global changeES) LandCover6k initiative¹.

5 Data availability

The database containing the reconstructions of coniferous forest, broadleaved forest and unforested land, three fractions of land cover, for the three time-periods presented in this paper, along with reconstructions for 1425 CE and 1000 BCE using only the K-LES_M are available for download from <https://github.com/BehnazP/SpatioCompo>. In addition the source code is available in the same repository under the open source GNU General Public License.

Acronyms

DVM	Dynamical vegetation model.
ALCC	Anthropogenic land-cover change.
PbLCC	Pollen based land-cover composition.
LPJ-GUESS	The Lund-Potsdam-Jena General Ecosystem Simulator, a DVM.
EFI-FM	European Forest Institute forest map.

Notation

Y_{PbLCC}	Observations, as proportions.
f	Link function, transforming between proportions and linear predictor.
η	Linear predictor, $\eta = \mu + \mathbf{X}$.
μ	Mean structure; modelled as $\mu = \mathbf{B}\beta$ using covariates, \mathbf{B} , and regression coefficients, β .
\mathbf{X}	Spatially dependent random effect.
α	Concentrated parameter of the Dirichlet distribution (i.e. observational uncertainty)
Σ	Covariance matrix that determines the variation between and within fields
κ	Scale parameter controlling the range of spatial dependency

¹www.pastglobalchanges.org/ini/wg/landcover6k/intro

Acknowledgements

The research presented in this paper is a contribution to the two Swedish strategic research areas Biodiversity and Ecosystems in a Changing Climate (BECC), and Modelling the Regional and Global Earth system (MERGE). The paper is also a contribution to PAGES LandCover6k. Lindström has been funded by Swedish Research Council (SRC, Vetenskapsrådet) grant no 2012-5983. Poska has been funded by SRC grant no 2016-03617 and the Estonian Ministry of Education grant IUT1-8. The authors would like to acknowledge Marie-José Gaillard for her efforts in providing the pollen based land-cover proxy data and thank her for valuable comments on this manuscript.

References

- J. Aitchison. *The statistical analysis of compositional data*. Chapman & Hall, Ltd., 1986.
- J. Aitchison, C. Barceló-Vidal, J. Martín-Fernández, and V. Pawlowsky-Glahn. Logratio analysis and compositional distance. *Math. Geol.*, 32(3):271–275, 2000.
- A. Arneeth, S. P. Harrison, S. Zaehle, K. Tsigaridis, S. Menon, P. J. Bartlein, J. Feichter, A. Korhola, M. Kulmala, D. O’donnell, et al. Terrestrial biogeochemical feedbacks in the climate system. *Nature Geosci.*, 3(8):525–532, 2010. doi: 10.1038/ngeo905.
- J. J. Becker, D. T. Sandwell, W. H. F. Smith, J. Braud, B. Binder, J. Depner, D. Fabre, J. Factor, S. Ingalls, S. H. Kim, R. Ladner, K. Marks, S. Nelson, A. Pharaoh, G. Sharman, R. Trimmer, J. VonRosenburg, G. Wallace, and P. Weatherall. Global bathymetry and elevation data at 30 arc seconds resolution: SRTM30_PLUS. *Marine Geol.*, 32(4):355–371, 2009.
- M. Blangiardo and M. Cameletti. *Spatial and Spatio-temporal Bayesian Models with R-INLA*. Wiley, 2015.
- S. Brooks, A. Gelman, G. L. Jones, and X.-L. Meng. *Handbook of Markov Chain Monte Carlo*. CRC Press, 2011.
- V. Brovkin, J. Bendtsen, M. Claussen, A. Ganopolski, C. Kubatzki, V. Petoukhov, and A. Andreev. Carbon cycle, vegetation, and climate dynamics in the holocene: Experiments with the CLIMBER-2 model. *Glob. Biogeochem. Cycles*, 16(4):1139, 2002.
- V. Brovkin, M. Claussen, E. Driesschaert, T. Fichefet, D. Kicklighter, M. Loutre, H. Matthews, N. Ramankutty, M. Schaeffer, and A. Sokolov. Biogeophysical effects of historical land cover changes

- simulated by six Earth system models of intermediate complexity. *Clim. Dyn.*, 26(6):587–600, 2006. doi: 10.1007/s00382-005-0092-6.
- W. L. Chapman and J. E. Walsh. Simulations of Arctic temperature and pressure by global coupled models. *J. Clim.*, 20(4):609–632, 2007. doi: 10.1175/JCLI4026.1.
- N. Christidis, P. A. Stott, G. C. Hegerl, and R. A. Betts. The role of land use change in the recent warming of daily extreme temperatures. *Geophys. Res. Lett.*, 40(3):589–594, 2013. doi: 10.1002/grl.50159.
- M. Claussen, V. Brovkin, and A. Ganopolski. Biogeophysical versus biogeochemical feedbacks of large-scale land cover change. *Geophys. Res. Lett.*, 28(6):1011–1014, 2001.
- H. J. de Knegt, F. van Langevelde, M. B. Coughenour, A. K. Skidmore, W. F. de Boer, I. M. A. Heitkönig, N. M. Knox, R. Slotow, C. van der Waal, and H. H. T. Prins. Spatial autocorrelation and the scaling of species–environment relationships. *Ecology*, 91(8):2455–2465, 2010. doi: 10.1890/09-1359.1.
- N. de Noblet-Ducoudré, J.-P. Boisier, A. Pitman, G. Bonan, V. Brovkin, F. Cruz, C. Delire, V. Gayler, B. van den Hurk, P. Lawrence, M. K. van der Molen, C. Müller, C. H. Reick, B. J. Strengers, , and A. Voldoire. Determining robust impacts of land-use-induced land cover changes on surface climate over North America and Eurasia: results from the first set of LUCID experiments. *J. Clim.*, 25(9): 3261–3281, 2012. doi: 10.1175/JCLI-D-11-00338.1.
- R. M. Fyfe, J. Woodbridge, and N. Roberts. From forest to farmland: pollen-inferred land cover change across Europe using the pseudobiomization approach. *Glob. Change Biol.*, 21(3):1197–1212, 2015. doi: 10.1111/gcb.12776.
- M.-J. Gaillard, S. Sugita, F. Mazier, A.-K. Trondman, A. Brostrom, T. Hickler, J. O. Kaplan, E. Kjellström, U. Kokfelt, P. Kuneš, , C. Lemmen, P. Miller, J. Olofsson, A. Poska, M. Rundgren, B. Smith, G. Strandberg, R. Fyfe, A. Nielsen, T. Alenius, L. Balakauskas, L. Barnekov, H. Birks, A. Bjune, L. Björkman, T. Giesecke, K. Hjelle, L. Kalnina, M. Kangur, W. van der Knaap, T. Koff, P. Lagerås, M. Latałowa, M. Leydet, J. Lechterbeck, M. Lindbladh, B. Odgaard, S. Peglar, U. Segerström, H. von Stedingk, and H. Seppä. Holocene land-cover reconstructions for studies on land cover-climate feedbacks. *Clim. Past*, 6:483–499, 2010.
- A. Gelfand, P. J. Diggle, P. Guttorp, and M. Fuentes. *Handbook of spatial statistics*. CRC Press, 2010.
- A. Gelman, J. B. Carlin, H. S. Stern, D. Dunson, A. Vehtari, and D. B. Rubin. *Bayesian Data Analysis*. Chapman & Hall/CRC, third edition, 2014.

- R. M. Gladstone, I. Ross, P. J. Valdes, A. Abe-Ouchi, P. Braconnot, S. Brewer, M. Kageyama, A. Kitoh, A. Legrande, O. Marti, O. R., O.-B. B., P. W. R., and V. G. Mid-Holocene NAO: A PMIP2 model intercomparison. *Geophys. Res. Lett.*, 32(16):L16707, 2005. doi: 10.1029/2005GL023596.
- K. K. Goldewijk, A. Beusen, G. Van Drecht, and M. De Vos. The HYDE 3.1 spatially explicit database of human-induced global land-use change over the past 12,000 years. *Glob. Ecol. Biogeogr.*, 20(1): 73–86, 2011.
- S. P. Harrison, P. J. Bartlein, S. Brewer, I. C. Prentice, M. Boyd, I. Hessler, K. Holmgren, K. Izumi, and K. Willis. Climate model benchmarking with glacial and mid-Holocene climates. *Clim. Dyn.*, 43 (3–4):671–688, 2014. doi: 10.1007/s00382-013-1922-6.
- T. Hastie, R. Tibshirani, and J. Friedman. *The Elements of Statistical Learning*. Springer Series in Statistics. Springer New York Inc., New York, NY, USA, 2001.
- G. B. M. Heuvelink, P. A. Burrough, and A. Stein. Propagation of errors in spatial modelling with GIS. *Int. J. Geogr. Inf. Syst.*, 3(4):303–322, 1989. doi: 10.1080/02693798908941518.
- T. Hickler, K. Vohland, J. Feehan, P. A. Miller, B. Smith, L. Costa, T. Giesecke, S. Fronzek, T. R. Carter, W. Cramer, I. Kühn, and M. T. Sykes. Projecting the future distribution of European potential natural vegetation zones with a generalized, tree species-based dynamic vegetation model. *Glob. Ecol. Biogeogr.*, 21(1):50–63, 2012. doi: 10.1111/j.1466-8238.2010.00613.x.
- J. O. Kaplan, K. M. Krumhardt, and N. Zimmermann. The prehistoric and preindustrial deforestation of Europe. *Quat. Sci. Rev.*, 28(27):3016–3034, 2009.
- T. Koenigk, L. Brodeau, R. G. Graversen, J. Karlsson, G. Svensson, M. Tjernström, U. Willén, and K. Wyser. Arctic climate change in 21st century CMIP5 simulations with EC-Earth. *Clim. Dyn.*, 40 (11-12):2719–2743, 2013. doi: 10.1007/s00382-012-1505-y.
- S. Kotz, N. Balakrishnan, and N. L. Johnson. *Continuous Multivariate Distributions. Volume 1: Models and Applications*. Wiley, 2000.
- F. Lindgren, H. Rue, and J. Lindström. An explicit link between Gaussian fields and Gaussian Markov random fields: the stochastic partial differential equation approach. *J. R. Stat. Soc. B*, 73(4):423–498, 2011. doi: 10.1111/j.1467-9868.2011.00777.x.
- E. Makalic and D. F. Schmidt. A simple sampler for the horseshoe estimator. *IEEE Signal Processing Lett.*, 23(1):179–182, 2016. doi: 10.1109/LSP.2015.2503725.

- U. Mikolajewicz, M. Gröger, E. Maier-Reimer, G. Schurgers, M. Vizcaíno, and A. M. Winguth. Long-term effects of anthropogenic CO₂ emissions simulated with a complex earth system model. *Clim. Dyn.*, 28(6):599–633, 2007. doi: 10.1007/s00382-006-0204-y.
- P. A. Miller and B. Smith. Modelling tundra vegetation response to recent arctic warming. *Ambio*, 41(3):281–291, 2012. doi: 10.1007/s13280-012-0306-1.
- J. Olofsson. *The Earth: climate and anthropogenic interactions in a long time perspective*. PhD thesis, Lund University, 2013. URL <http://lup.lub.lu.se/record/3732052>.
- T. Park and G. Casella. The bayesian lasso. *J. Am. Stat. Assoc.*, 103(482):681–686, 2008. doi: 10.1198/016214508000000337.
- B. Pirzamanbein, J. Lindström, A. Poska, S. Sugita, A.-K. Trondman, R. Fyfe, F. Mazier, A. Nielsen, J. Kaplan, A. Bjune, H. Birks, T. Giesecke, M. Kangur, M. Latałowa, L. Marquer, B. Smith, and M.-J. Gaillard. Creating spatially continuous maps of past land cover from point estimates: A new statistical approach applied to pollen data. *Ecol. Complex.*, 20:127–141, 2014. doi: 10.1016/j.ecocom.2014.09.005.
- B. Pirzamanbein, J. Lindström, A. Poska, and M.-J. Gaillard. Modelling spatial compositional data: Reconstructions of past land cover and uncertainties. *Spatial Stat.*, 24:14–31, 2018. doi: 10.1016/j.spasta.2018.03.005.
- A. Pitman, N. de Noblet-Ducoudré, F. Cruz, E. Davin, G. Bonan, V. Brovkin, M. Claussen, C. Delire, L. Ganzeveld, V. Gayler, B. J. J. M. van den Hurk, P. J. Lawrence, M. K. van der Molen, C. Mller, C. H. Reick, S. I. Seneviratne, B. J. Strengers, and A. Voltaire. Uncertainties in climate responses to past land cover change: First results from the LUCID intercomparison study. *Geophys. Res. Lett.*, 36(14):n/a–n/a, 2009. doi: 10.1029/2009GL039076.
- R. Pivinen, M. Lehtikoinen, A. Schuck, T. Hme, S. Vtinen, P. Kennedy, and S. Folving. Combining Earth observation data and forest statistics. Technical Report 14, European Forest Institute, Joint Research Centre-European Commission., 2001. URL <https://www.efi.int/publications-bank/combining-earth-observation-data-and-forest-statistics>. ISBN: 952-9844-84-0 ISSN: 1238-8785.
- J. Pongratz, C. Reick, T. Raddatz, and M. Claussen. A reconstruction of global agricultural areas and land cover for the last millennium. *Glob. Biogeochem. Cycles*, 22(3):GB3018, 2008. doi: 10.1029/2007GB003153.

- I. C. Prentice, A. Bondeau, W. Cramer, S. P. Harrison, T. Hickler, W. Lucht, S. Sitch, B. Smith, and M. T. Sykes. Dynamic global vegetation modeling: quantifying terrestrial ecosystem responses to large-scale environmental change. In J. G. Canadell, D. E. Pataki, and L. F. Pitelka, editors, *Terrestrial Ecosystems in a Changing World. Global Change — The IGBP Series*, pages 175–192. Springer, 2007. doi: 10.1007/978-3-540-32730-1_15.
- J. A. Richter-Menge, M. O. Jeffries, and J. E. Overland, editors. *Arctic Report Card 2011*. National Oceanic and Atmospheric Administration, 2011. URL www.arctic.noaa.gov/reportcard.
- H. Rue and L. Held. *Gaussian Markov Random Fields; Theory and Applications*, volume 104 of *Monographs on Statistics and Applied Probability*. Chapman & Hall/CRC, 2005.
- P. Samuelsson, C. G. Jones, U. Willén, A. Ullerstig, S. Gollvik, U. Hansson, C. Jansson, E. Kjellström, G. Nikulin, and K. Wyser. The Rossby Centre regional climate model RCA3: model description and performance. *Tellus A*, 63(1):4–23, 2011.
- S. Scheiter, L. Langan, and S. I. Higgins. Next-generation dynamic global vegetation models: learning from community ecology. *New Phytologist*, 198(3):957–969, 2013. doi: 10.1111/nph.12210.
- A. Schuck, J. van Brusselen, R. Päivinen, T. Häme, P. Kennedy, and S. Folving. Compilation of a calibrated European forest map derived from NOAA-AVHRR data. EFI Internal Report 13, EuroForIns, 2002.
- S. Sitch, B. Smith, I. C. Prentice, A. Arneth, A. Bondeau, W. Cramer, J. Kaplan, S. Levis, W. Lucht, M. Sykes, K. Thonicke, and S. Venevsky. Evaluation of ecosystem dynamics, plant geography and terrestrial carbon cycling in the LPJ dynamic global vegetation model. *Glob. Change Biol.*, 9(2): 161–185, 2003.
- B. Smith, I. C. Prentice, and M. T. Sykes. Representation of vegetation dynamics in the modelling of terrestrial ecosystems: comparing two contrasting approaches within European climate space. *Glob. Ecol. Biogeogr.*, 10:621–637, 2001.
- G. Strandberg, J. Brandefelt, E. Kjellström, and B. Smith. High-resolution regional simulation of last glacial maximum climate in Europe. *Tellus A*, 63(1):107–125, 2011.
- G. Strandberg, E. Kjellström, A. Poska, S. Wagner, M.-J. Gaillard, A.-K. Trondman, A. Mauri, B. A. S. Davis, J. O. Kaplan, H. J. B. Birks, A. E. Bjune, R. Fyfe, T. Giesecke, L. Kalnina, M. Kangur, W. O. van der Knaap, U. Kokfelt, P. Kuneš, M. Latał owa, L. Marquer, F. Mazier, A. B. Nielsen,

- B. Smith, H. Seppä, and S. Sugita. Regional climate model simulations for Europe at 6 and 0.2 kbp: sensitivity to changes in anthropogenic deforestation. *Clim. Past*, 10(2):661–680, 2014. doi: 10.5194/cp-10-661-2014. URL <http://www.clim-past.net/10/661/2014/>.
- A.-K. Trondman, M.-J. Gaillard, S. Sugita, F. Mazier, R. Fyfe, J. Lechterbeck, L. Marquer, A. Nielsen, C. Twiddle, P. Barratt, H. Birks, A. Bjune, C. Caseldine, R. David, J. Dodson, W. Dörfler, E. Fischer, T. Giesecke, T. Hultberg, M. Kangur, P. Kuneš, M. Latałowa, M. Leydet, M. Lindbalddh, F. Mitchell, B. Odgaard, S. Peglar, T. Persson, M. Rösch, P. van der Knaap, B. van Geel, A. Smith, and L. Wick. Pollen-based quantitative reconstructions of past land-cover in NW Europe between 6k years BP and present for climate modelling. *Glob. Change Biol.*, 21(2):676–697, 2015. doi: 10.1111/gcb.12737.
- W. Zhang, P. A. Miller, B. Smith, R. Wania, T. Koenigk, and R. Döscher. Tundra shrubification and tree-line advance amplify arctic climate warming: results from an individual-based dynamic vegetation model. *Environ. Res. Lett.*, 8(3):034023, 2013.